*2024 IEEE Applied Power Electronics Conference and Exposition (APEC)*

# Stability Analysis of Second-Order Harmonic Active Filters for Input-Series/Output-Parallel Solid State Transformers

A. Cervone, T. Wei, and D. Dujic



POWER ELECTRONICS LABORATORY
ÉCOLE POLYTECHNIQUE FÉDÉRALE DE LAUSANNE

# Stability Analysis of Second-Order Harmonic Active Filters for Input-Series/Output-Parallel Solid State Transformers

Andrea Cervone, Tianyu Wei, and Drazen Dujic
Power Electronics Laboratory - PEL
École Polytechnique Fédérale de Lausanne - EPFL
Lausanne, CH-1015, Switzerland
andrea.cervone@epfl.ch, tianyu.wei@epfl.ch, drazen.dujic@epfl.ch

***Abstract*—Solid-State Transformers with Input-Series/Output-Parallel configuration offer a convenient solution for AC/DC power conversion, thanks to their modularity, scalability and flexibility. However, as known, they are affected by a second-order harmonic ripple due to a local single-phase AC/DC conversion in each module. This ripple can be counteracted by installing Active Power Filters, eliminating the need for oversized DC-bus capacitances. However, in an ISOP SST, dynamic interactions may arise from the coupling between different modules. This paper analyzes their effect on the stability of the APFs. It is shown that achieving stability for a single APF individually is not sufficient to guarantee the stability when multiple units are operated at once, but instead stronger requirements are needed. The analysis is supported by experimental validation, and the results can aid to improve the robustness of future SST designs.**

***Index Terms*—Input-Series/Output-Parallel (ISOP), Solid-State Transformer (SST), Active Power Filter (APF), Active Power Decoupling, Stablility.**

## I. Introduction

SOLID State Transformers (SSTs) are power electronics converters aiming at offering the same characteristics as traditional transformers, being voltage/current scaling and galvanic insulation, but with enhanced controllability and with the extension to also DC/DC and AC/DC systems [1].

A flexible and highly scalable SST architecture is the Input-Series/Output-Parallel (ISOP) configuration, that features multiple identical conversion units connected in series on the primary side to attain high voltage ratings, and in parallel on the secondary side to attain high current ratings [1]–[3]. An example of an ISOP SST architecture is shown in Fig. 1 (discussed in [4]), which is taken as a specific application example for the analysis and derivations of this work.

When an ISOP SST is employed for AC/DC conversion, each module normally employs a dedicated single-phase AC/DC conversion stage. However, as known, a single phase AC/DC conversion stage introduces to the corresponding DC-bus a power oscillation at twice the AC grid frequency. This, in turn, leads to a second-order harmonic ripple affecting the DC-bus of all the modules of the SST [5]. This issue is also present in ISOP SSTs employed for a three-phase AC grid, since they are normally implemented as three separate single-phase branches.

The second-order harmonic ripple can be neutralized through active power filters (APFs): additional conversion structures that can store the fluctuating energy in ad-hoc designed buffering elements, removing the need for oversized DC-bus capacitances or bulky passive trap filters [6]–[8].

Each APF, once installed into an SST module, should ideally operate to fight the ripple on the corresponding DC-bus voltage. However, in ISOP configurations, the SST modules are dynamically coupled, and an APF can also affect other modules. The mutual interaction has been first discussed in [9] regarding the effects on the steady-state operating conditions of the system. It has been shown that the interconnection of the SST modules can induce resonances within the system, which may affect the steady-state distribution of the second-order harmonic ripple between the SST modules, according to different operating modes of the APFs.

This work, instead, analyzes the mutual interactions in the SST from a different perspective, by investigating the dynamical performances with a specific focus on the system stability. In what follows, it will be shown that, even if each individual APF is designed to guarantee a stable operation when installed in the SST, some instabilities may occur when multiple APF units are activated simultaneously. This means that the stability of a single APF unit is not sufficient to guarantee the stability of the overall system, and that instead stronger requirements must be met.

To explain this unexpected behavior, a model of the interactions existing within an ISOP SST is here derived, by considering the SST as a multi-port circuit that can be analyzed in the Laplace domain through its corresponding impedances matrix. In this framework, the interaction between different modules is represented by the mutual impedances of the network, and the insurgence of instabilities can be motivated by the different distribution of the closed-loop poles of the system when multiple APFs are interacting with the SST.

The results of this study can be used to improve the design of ISOP SSTs and of APFs, with the aim of guaranteeing more robust and reliable systems.

979-8-3503-1664-3/24/$31.00 ©2024 IEEE

## II. Analyzed Setup

The analysis of this work is based on a specific case study, but the results can be generalized to other similar structures.

The analyzed ISOP SST architecture is the low voltage prototype of the Power Electronic Traction Transformer (LV PETT) described in [4] and represented in Fig. 1. This converter was originally developed by ABB as an analog simulator with modest power ratings for control hardware and software verification of a corresponding medium voltage demonstrator (MV PETT, described in [10]), and it has been generously donated to the Power Electronics Laboratory (PEL) of the École Polytechnique Fédérale de Lausanne (EPFL), where it is currently used as an SST research platform.

The circuit architecture of the PETT, represented in Fig. 1, is composed of $N = 9$ identical modules, each of which includes a two-stage conversion circuit, with a non-isolated AC/DC stage and a galvanically isolated DC/DC stage.

The AC/DC conversion stages are based on a full-bridge architecture. They are operated in closed-loop to control the AC grid current in a way to transfer, with unitary power factor, a desired power flow. The transferred power is itself obtained from a closed-loop controller with the aim of stabilizing the DC-bus voltage on the secondary side of the overall SST. A phase shift pulse width modulation is implemented to control the full-bridge converters. By shifting the carrier of the 9 modules by $1/9$ of their period, it is possible to improve the harmonic content of the equivalent voltage generated on the AC side, despite the relatively low switching frequency. At the same time, the switching harmonics generated by the AC/DC converters on the DC-bus currents of the 9 modules, once combined at the parallel output of the ISOP structure, cancel one another, meaning that the switching harmonics do not propagate to the secondary side of the SST [4], [10], [12].

The isolated DC/DC conversion stages are realized with an LLC series resonant conversion topology, implemented with a half-bridge leg and a split-capacitor. The primary-side half-bridge legs are operated in open-loop with a $50\%$ duty-cycle modulation at a frequency slightly lower than the resonance frequency of the LLC tank, in order to achieve soft-switching operation [4], [10], [11].

A Buck-type active power filter has been installed in each of the 9 floating DC-buses of the PETT, as represented in the circuit diagram of Fig. 1. The aim of the APFs is to counteract the second-order harmonic ripple introduced by the AC/DC conversion stages of each SST module. This is done by locally storing in the buck capacitance a fluctuating energy, that oscillates at twice the AC grid frequency in a way to eliminate the power fluctuation from the DC-bus. The magnitude and phase angle of this fluctuating energy is locally computed in each APF unit by a feedback controller aimed at neutralizing the second-order harmonic ripple from the corresponding DC-bus voltage. Additional details about the adopted active power filters can be found in [9], [12], [13].

As described in [12], the presence of the APFs allowed the reduction of the primary-side DC-bus capacitance of each ISOP module from $4\,\mathrm{mF}$ to $375\,\mu\mathrm{F}$. Indeed, thanks to the APFs, the DC-bus capacitances do not need to be sized for the suppression of the second-order harmonic ripple, and is instead only subject to the switching harmonics produced by the conversion stages of the SST. Additionally, compared to [9], [12], [13], in this work the secondary-side DC-bus capacitances have also been reduced, from $2.35\,\mathrm{mF}$ to $680\,\mu\mathrm{F}$.

The used parameters of the LV PETT and of the APFs are summarized in Table I.

## III. Stability of the APFs in the ISOP SST

The analysis of this work takes origin from experimental observation of unstable behavior of multiple APF units working simultaneously in the SST.

After the reduction of the DC-bus capacitances of the LV PETT compared to previous works, the controller of the APF has been modified and tuned again to take into account the changes in the system parameters. Following these changes, a single APF unit, installed in the module 1 of the SST, has been tested again on the LV PETT to verify the stable behavior.

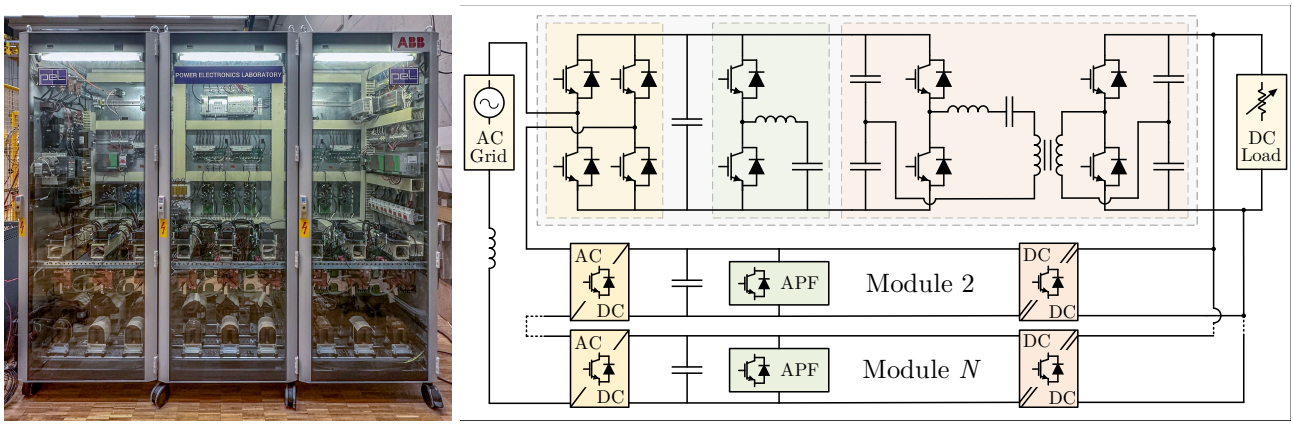


Fig. 1. The Power Electronics Traction Transformer (PETT), analyzed as example of an ISOP SST: Left) Experimental setup; Right) Circuit Topology.

TABLE I
USED PARAMETERS OF THE PETT

| Parameter | | Value |
|---|---|---|
| Power | $P$ | 8 kW |
| AC Grid Voltage (RMS) | $V_{AC,RMS}$ | 800 V |
| AC Grid Frequency | $f_{AC}$ | 50 Hz |
| Number of ISOP Modules | $N$ | 9 |
| Primary DC Voltage (single module) | $V_{DC}$ | 220 V |
| Primary DC Capacitance (single module) | $C_{p,LLC}$ | 375 µF |
| Secondary DC Voltage | $V_{DC,out}$ | 220 V |
| Secondary DC Capacitance (equivalent) | $C_{s,LLC}$ | 680 µF |
| LLC Resonant Inductance | $L_{res}$ | 135 µH |
| LLC Resonant Capacitance | $C_{res}$ | 60 µF |
| LLC Magnetizing Inductance | $L_{mag}$ | 13 mH |
| LLC Transformation Ratio | $N_1/N_2$ | 1 |
| AC/DC Switching Frequency | $f_{AC/DC}$ | 317 Hz |
| DC/DC Switching Frequency | $f_{DC/DC}$ | 1.5 kHz |
| APF Apparent Power | $S_{APF}$ | 1 kVA |
| APF Inductance | $L_{APF}$ | 200 µH |
| APF Capacitance | $C_{APF}$ | 360 µF |
| APF Capacitor Voltage | $V_C^*$ | 160 V |
| APF DC-bus Capacitance | $C_{p,APF}$ | 120 µF |
| APF Switching Frequency | $f_{sw,APF}$ | 10 kHz |

An experimental recording confirming the proper operation of the APF is here reported in Fig. 2. The image shows the current $i_{APF,1}$ injected into the DC-bus of the SST module 1 APF, the DC-bus voltage $v_{DC,1}$ of the corresponding SST module, and the DC-bus voltage $v_{DC,2}$ of another SST module. The graphs on the left show the measured instantaneous variables, while the graphs on the right, denoted by the superscript $*^{\langle 2\rangle}$, represent the magnitude of their second-order harmonic component, computed through a time-moving Fourier decomposition over a time window of 50 ms, as described in [13].

As can be noted, after the APF activation, the current $i_{APF,1}$ increases, and a second-order harmonic component at 100 Hz is injected to the DC-bus of the ISOP SST module 1, which properly neutralizes the second order harmonic component in the DC-bus voltage $v_{DC,1}$ in around 1.5 s. The current $i_{APF,1}$ also slightly affects the other SST modules, and a small increase of the second-order harmonic ripple can be noted on $v_{DC,2}$. Similar effects are also encountered in the DC-bus voltages $\{v_{DC,3}, \ldots, v_{DC,9}\}$ of the remaining SST modules. This result confirmed, as desired, the stable behavior of the APF unit in the SST.

However, unexpected observations arose when multiple APFs were enabled at the same time. Indeed, in this case, it could be seen that the system was not working stably anymore, and after the activation of the APFs the relevant variables of the SST were quickly diverging to excessive values, causing the intervention of some protection in the system.

An example of this behavior is here reported in Fig. 3. In this test the SST was initially working in steady state operation with only one APF unit enabled (of the module 1), when the activation signal is sent to all the other 8 APF units installed in the PETT. As can be noted, quickly after the activation, all the relevant variables are quickly undergoing an exponential increase in the magnitude of their second-order harmonic component. This denotes a clear insurgence of an

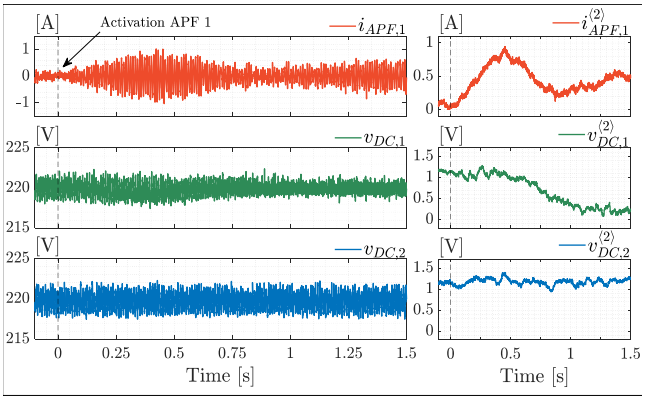


Fig. 2. Experimental results showing the activation of a single APF. The system is stable and the activation transient extinguishes in around 1.5 s.

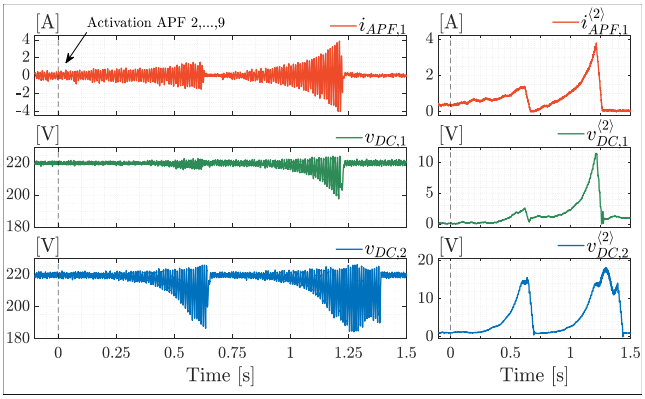


Fig. 3. Experimental results showing the activation of all APFs, starting from the steady state condition with only one APF in operation. The system is unstable and the variables increase exponentially until the intervention of the SST protection mechanisms.

unstable behavior, which is only interrupted by the protection mechanisms of the system causing the tripping of the APFs.

This unexpected result clearly shows that, even if one APF can work stably in the SST, the simultaneous operation of multiple APF units may result in instability. To properly explain and motivate this phenomenon, which should be carefully examined in the SST design stage, a proper modeling of the system is required, which is derived in the following sections.

## IV. ANALYSIS AND EXPLANATIONS

The experimental observations discussed in the previous section have shown that, even if a single APF unit is properly designed to guarantee stable operation by itself, it is not automatically guaranteed that it will keep working stably when multiple units are simultaneously operating in the SST.

This unexpected behavior needs to be properly considered when designing active power filters for an ISOP SST. This section is aimed at mathematically analyzing the system to provide clarification on this phenomenon. As shown in the following, the observed instability can be explained as an effect of the intrinsic mutual coupling existing among different modules of the system.

### A. Dynamical Model of the SST

To analyze the interactions between the APFs and the SST, it is first necessary to establish a proper model of the SST itself. In this perspective, it should be explicitly considered that different conversion stages in an ISOP configuration do not work independently, but can interact with one another and contribute to the dynamic behavior of all the relevant variables in each module.

Considering the LV PETT, in the small signal approximation, the overall behavior of the system can be analyzed by referring to the equivalent circuit represented in Fig. 4. In this equivalent circuit, initially developed in [9], the AC/DC stages are modeled as simple current sources injecting the second-order harmonic ripple to the system, the DC load is modeled as a purely resistive element, and the LLC conversion stages are modeled with a Π circuit consisting of two shunt capacitors and an ohmic-inductive branch. In this approach, each APF units can be also analyzed as equivalent current source, that can be controlled to inject a desired current into the corresponding DC-bus.

Considering the split-capacitor configuration of the analyzed system, the equivalent capacitances of each module are one half of the installed capacitance at the primary-side and secondary-side of the LLC converters. For the primary side, the equivalent capacitance $C_p$ takes also into account the contribution of the local DC-bus capacitance of the APF.

The equivalent inductance and resistance of the LLC converter identify the equivalent stored energy and the equivalent losses of the DC/DC conversion stage, respectively [14]. For a split-capacitor configuration they can be approximated as:

$$L_{DC} \approx L_{res} \cdot \left(\pi f_{res}/f_{sw,DC/DC}\right)^2 \tag{1}$$

$$R_{DC} \approx R_{res} \cdot \left(\pi^2/2\right) \cdot \left(f_{res}/f_{sw,DC/DC}\right) \tag{2}$$

with $R_{res}$ taking into account the overall resistance of the LLC converter, and $f_{res} = 1/(2\pi\sqrt{L_{res}C_{res}})$ being the resonance frequency of the converter [14]. In the considered setup, $L_{DC} \approx 1.85\,\mathrm{mH}$ and $R_{DC} \approx 1\,\Omega$.

Then, seen from the terminals of the APFs, the overall ISOP SST behaves as a linear multi-port circuit. Then, the dynamics of the DC-bus voltages can be mathematically formulated in the Laplace domain, and assuming all the SST modules to be identical they can be expressed as:

$$\underbrace{\begin{bmatrix} v_{DC,1} \\ v_{DC,2} \\ \vdots \\ v_{DC,N} \end{bmatrix}}_{\boldsymbol{v}_{DC}(s)} = \underbrace{\begin{bmatrix} v_r \\ v_r \\ \vdots \\ v_r \end{bmatrix}}_{\boldsymbol{v}_r(s)} - \underbrace{\begin{bmatrix} Z_A & Z_M & \cdots & Z_M \\ Z_M & Z_A & \cdots & Z_M \\ \vdots & \vdots & \ddots & \vdots \\ Z_M & Z_M & \cdots & Z_A \end{bmatrix}}_{\boldsymbol{Z}_{SST}(s)} \cdot \underbrace{\begin{bmatrix} i_{APF,1} \\ i_{APF,2} \\ \vdots \\ i_{APF,N} \end{bmatrix}}_{\boldsymbol{i}_{APF}(s)} \tag{3}$$

where $v_r$ represents the ripple that would be present in each DC-bus voltage when the APF units are disabled, and $\boldsymbol{Z}_{SST}(s)$ is an impedance matrix linking the effects of the APF currents $\{i_{APF,1}, \ldots, i_{APF,N}\}$ on the DC-bus voltages $\{v_{DC,1}, \ldots, v_{DC,N}\}$.

As can be noted, because of the assumed equivalence of the SST modules, the matrix $\boldsymbol{Z}_{SST}(s)$ is symmetrical, and $Z_A(s)$ represents the equivalent impedance seen by one APF unit, while $Z_M(s)$ describes the mutual interaction between different SST modules. Their analytical expressions are reported in (4)-(5), while their Bode diagrams are represented in Fig. 5 referring to the values of Table I. With the considered parameters, a resonance effect can be observed close to 200 Hz, caused by the interaction between the equivalent inductances of the LLC model and the DC-bus capacitances.

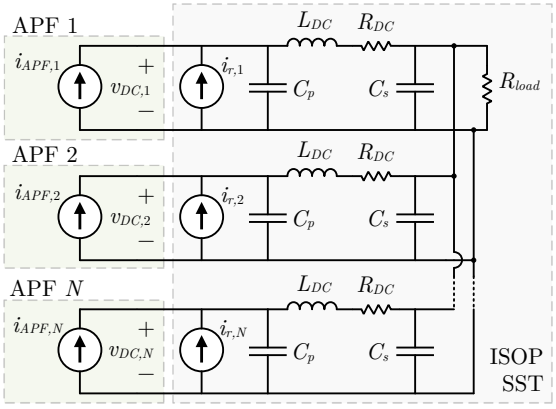


Fig. 4. Simplified equivalent circuit to analyze the LV PETT.

### B. Effect of the Mutual Coupling in the ISOP SST on the Open-Loop Operation of the APFs

The presence of the mutual coupling effect on the SST, identified by the mutual impedance $Z_M(s)$, can influence the behavior of the APF units connected to the system.

To verify this effect in the LV PETT, the system has been first tested by activating the APFs in open-loop, externally commanding them to inject a constant second-order harmonic current corresponding to the same current injected by the

$$Z_A(s) = \cfrac{1}{sC_p + \cfrac{1}{sL_{DC} + R_{DC} + \cfrac{1}{(N-1)/Z_b(s) + N\,sC_s + 1/R_{load}}}} \quad \text{with} \quad Z_b(s) = sL_{DC} + R_{DC} + \frac{1}{sC_p} \tag{4}$$

$$Z_M(s) = Z_A(s) \cdot \frac{1/sC_p}{Z_b(s)} \cdot \frac{1}{(N-1)/Z_b(s) + N\,sC_s + 1/R_{load}} \cdot \cfrac{1}{sL_{DC} + R_{DC} + \cfrac{1}{(N-1)/Z_b(s) + N\,sC_s + 1/R_{load}}} \tag{5}$$

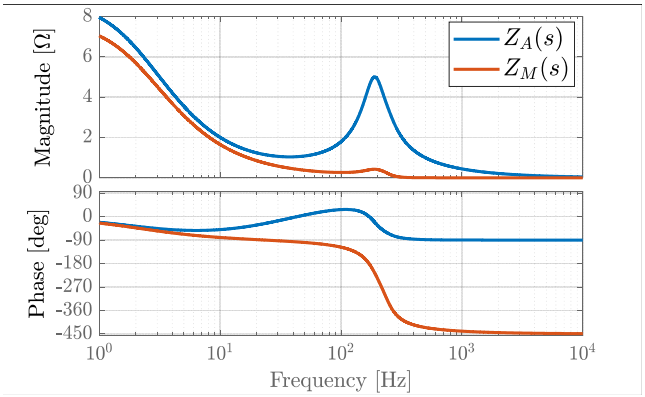


Fig. 5. Magnitude and phase diagram of the self-impedance $Z_A(s)$ and of the mutual impedance $Z_M(s)$ of the PETT for varying frequency, considering nominal loading conditions.

AC/DC stages, without any feedback based on their measured DC-bus voltage. Ideally, with this external reference, the current injected by each APF unit should compensate the current injected by the AC/DC stage in the same DC-bus, which should lead to the complete neutralization of the corresponding DC-bus voltage ripple.

The results of these tests are shown in Fig. 6 and in Fig. 7, respectively considering the case when only when all 9 APFs unit are simultaneously activated, and when instead only one APF unit is in operation. The results show the instantaneous variables (left columns), the magnitude of the time-moving second-order harmonic components (right columns) and the value of coefficients of the same harmonic components (center columns, with the cosine and sine coefficients respectively denoted by the superscripts $*^{\langle 2c \rangle}$ and $*^{\langle 2s \rangle}$, as done in [13]).

As can be noted, the effect of activating only one APF individually and of activating all APFs at the same time is completely opposite.

Indeed, when all the APF units are simultaneously working (as in Fig. 6), the cancellation of the currents injected by the AC/DC stages lead, as expected, to a decrease of the second-order harmonic ripple $v^{\langle 2 \rangle}_{DC,1}$ and $v^{\langle 2 \rangle}_{DC,2}$ on the DC-bus voltages (which is almost completely neutralized).

Instead, when only one APF unit is activated, the cancellation of the current injected by only one AC/DC stage unexpectedly leads to an increase of the second-order harmonic ripple of the corresponding DC-bus voltage $v^{\langle 2 \rangle}_{DC,1}$, while a slightly reduction can be noted on $v^{\langle 2 \rangle}_{DC,2}$.

This is the direct effect of the mutual coupling among the SST modules, and is in line with the expected behavior that can be obtained from the theoretical impedances shown in Fig. 5. Indeed, if the SST modules were not coupled, the neutralization of the second-order harmonic current injected by an AC/DC conversion stage in the test of Fig. 7 would have lead to a decrease in the ripple $v^{\langle 2 \rangle}_{DC,1}$ of the corresponding DC-bus voltage, and it would have had no effect on the ripple $v^{\langle 2 \rangle}_{DC,2}$ on another SST module.

Instead, since the mutual coupling is not negligible, each SST module is not only affected by a second-order harmonic current introduced by the corresponding AC/DC conversion stage, but is also affected by an additional second-order ripple coming from the AC/DC stages in the other 8 modules, which is transferred to the DC-bus through the DC/DC stage. Therefore, when a single APF is activated in open-loop, it can neutralize the effect of the AC/DC stage, but it cannot neutralize this additional term coming from the other modules. As seen in the provided example, this could even lead to an increase in the DC-bus voltage ripple.

### C. Effect of the Mutual Coupling in the ISOP SST on the Closed-Loop Operation of the APFs

From the previous analysis it has been shown that the mutual coupling existing in the SST can affect the behavior of the APF units, even when they are operated in open-loop. In closed-loop operation, this effect could be emphasized and self-sustained, which may lead to the insurgence of unstable condition as previously shown in Section III.

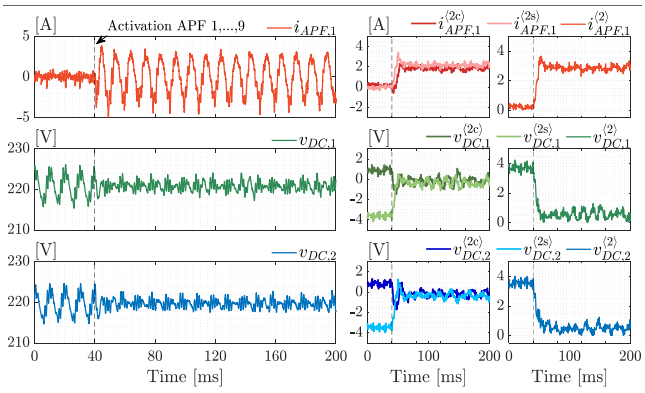


Fig. 6. Experimental results showing the open-loop activation of all APF units, used to observe the cumulative effect of multiple APFs in the SST, which results from combination of both $Z_A$ and $Z_M$.

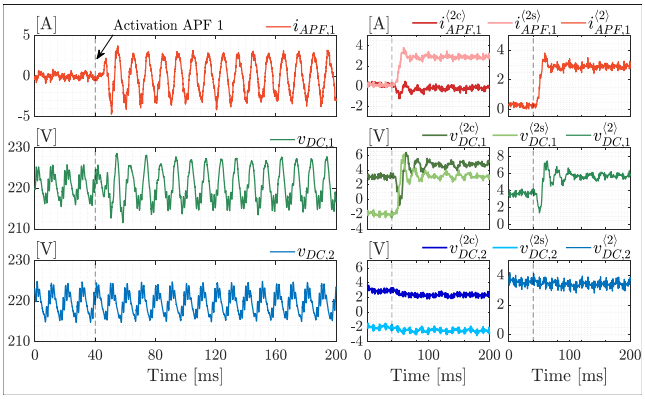


Fig. 7. Experimental results showing the open-loop activation of a single APF, used to observe the effect of the self-impedance $Z_A$ and of the mutual-impedances $Z_M$ in the ISOP SST.

To analyze this phenomenon, it is possible to model the effect of the closed-loop operation of the APFs on the SST, in a way to investigate their interaction.

In closed-loop operation, each APF is locally controlled to inject a current $i_{APF,k}$ computed from the measured DC-bus voltage $v_{DC,k}$. This relationship can be mathematically formalized as:

$$i_{APF,k}(s) = Y_{APF}(s) \cdot v_{DC,k}(s) \tag{6}$$

and $Y_{APF}(s)$ represents the equivalent admittance of the APF, which depends on its control algorithm.

When only a single APF is enabled, the dynamics of the corresponding DC-bus voltage is:

$$\begin{aligned} v_{DC,k}(s) &= v_r(s) - Z_A(s) \cdot i_{APF,k}(s) = \\ &= v_r(s) - Z_A(s) \cdot Y_{APF}(s) \cdot v_{DC,k}(s) \end{aligned} \tag{7}$$

meaning that the voltage $v_{DC,k}$ on the corresponding DC-bus terminals is given by

$$v_{DC,k}(s) = \underbrace{\frac{1}{1 + Z_A(s) \cdot Y_{APF}(s)}}_{S_{APF}(s)} \cdot v_r(s) \tag{8}$$

and the closed-loop stability depends on the relationship between $Z_A(s)$ and $Y_{APF}(s)$. The stability can be achieved by designing $Y_{APF}(s)$ in a way that $Z_A(s) \cdot Y_{APF}(s)$ satisfies the Nyquist stability criterion.

On the contrary, when all the APFs are enabled simultaneously, the DC-bus voltages evolve as:

$$\begin{aligned} \boldsymbol{v}_{DC}(s) &= \boldsymbol{v}_r(s) - \boldsymbol{Z}_{SST}(s) \cdot \boldsymbol{i}_{APF}(s) = \\ &= \boldsymbol{v}_r(s) - \boldsymbol{Z}_{SST}(s) \cdot \boldsymbol{Y}_{APF}(s) \cdot \boldsymbol{v}_{DC}(s) \end{aligned} \tag{9}$$

which can be rearranged to get

$$\boldsymbol{v}_{DC}(s) = \underbrace{\left[\boldsymbol{I} + \boldsymbol{Z}_{SST}(s) \cdot \boldsymbol{Y}_{APF}(s)\right]^{-1}}_{\boldsymbol{S}(s)} \cdot \boldsymbol{v}_r(s) \tag{10}$$

In this case, the closed loop stability depends on the transfer matrix $\boldsymbol{S}(s) = \left[\boldsymbol{I} + \boldsymbol{Z}_{SST}(s) \cdot \boldsymbol{Y}_{APF}(s)\right]^{-1}$. Given the symmetry properties of the SST impedance matrix $\boldsymbol{Z}_{SST}(s)$, also the transfer matrix $\boldsymbol{S}(s)$ is symmetric, and with identical diagonal and non-diagonal terms. It can be expressed as:

$$\boldsymbol{S}(s) = \begin{bmatrix} S_A & S_M & \cdots & S_M \\ S_M & S_A & \cdots & S_M \\ \vdots & \vdots & \ddots & \vdots \\ S_M & S_M & \cdots & S_A \end{bmatrix} \tag{11}$$

and the analytical expressions of $S_A(s)$ and $S_M(s)$ are given in (12)-(13).

To guarantee the stability, both $S_A(s)$ and $S_M(s)$ should be stable at the same time, meaning that all their poles should be located on the left-half domain of the complex plane. However, as can be noted, their expressions depend not only on $Z_A(s)$ and $Y_{APF}(s)$, but also on $N$ and $Z_M(s)$.

If $Z_M(s) = 0$, it would be easy to show from (12)-(13) that $S_A(s) = S_{APF}(s)$ (with $S_{APF}(s)$ given by (8)), and that $S_M(s) = 0$. This would mean that all the SST modules would be perfectly decoupled, and the stable operation of a single APF would be enough to guarantee a stable operation when all APFs are simultaneously operating.

However, because of the mutual coupling between the SST modules, the impedance $Z_M(s)$ is different from 0, and the poles of $S_A(s)$ and $S_M(s)$ differ from the poles of $S_{APF}(s)$. To be more specific, by observing (12)-(13), it can be deduced that the more the SST modules are coupled (i.e., the higher is $|Z_M(s)|$ compared to $|Z_A(s)|$), and the higher is the total number of modules $N$ of the SST, the more the distribution of the poles is changed.

Therefore, the closed-loop stability of the overall system cannot be inferred from the closed loop stability of a single active power filter in operation. These results can be used to explain the aforementioned insurgence of instabilities in the PETT, previously described in Section III. In the previously shown experiments, the controller implemented in the APF could be approximately described by the transfer function:

$$Y_{APF}(s) = \frac{sK_1 - s^2K_2}{s^2 + \omega_0^2} \tag{14}$$

with $K_1 = 2.5$, $K_2 = 4 \cdot 10^{-3}$ and $\omega_0 = 2\pi 100$.

It is possible to analyze the distribution of the closed loop poles of $S_{APF}(s)$ (computed from (8)) and compare them with the poles of $S_A(s)$ and $S_M(s)$ (computed from (12)-(13)). The results, computed numerically in the MATLAB environment, are shown in Fig. 8. As can be seen, the location of the poles is sensibly modified when all APFs are in operation, and while all the poles of $S_{APF}(s)$ are located in the left-half side of the complex plane, both $S_A(s)$ and $S_M(s)$ have a pair of complex conjugate poles in the right-half side, which explain the observed system instability.

Based on these considerations, the tuning of the APF controller can be properly modified to take into account the effect of the mutual coupling existing in the SST, in a way to enforce the stable behavior even when all the APF units are operated simultaneously.

An example is here given considering the same transfer function $Y_{APF}(s)$ given in (14), but with the modified gains $K_1 = 1.5$ and $K_2 = 0$. The distribution of the closed-loop

$$S_A(s) = \frac{[Y_{APF}Z_A + (N-2) \cdot Y_{APF}Z_M + 1]}{[1 + Y_{APF}Z_A] \cdot [Y_{APF}Z_A + (N-2) \cdot Y_{APF}Z_M + 1] - (N-1) \cdot [Y_{APF}Z_M]^2} \tag{12}$$

$$S_M(s) = \frac{-[Y_{APF}Z_M]}{[1 + Y_{APF}Z_A] \cdot [Y_{APF}Z_A + (N-2) \cdot Y_{APF}Z_M + 1] - (N-1) \cdot [Y_{APF}Z_M]^2} \tag{13}$$

(the explicit dependence of $Z_A$, $Z_M$ and $Y_{APF}$ on the Laplace complex variable $s$ has been omitted for notation compactness)

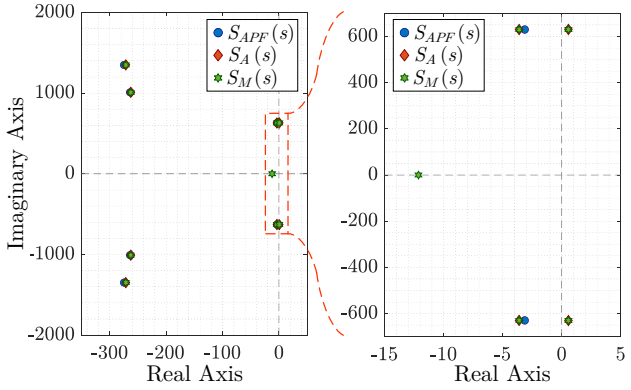


Fig. 8. Distribution of the poles in the closed-loop system considering the interaction between the SST and the APFs. Left) Distribution of all the poles in the complex plane; Right) Zoom around the imaginary axis.

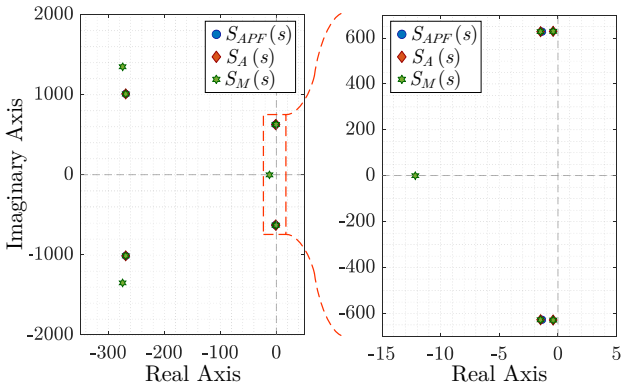


Fig. 9. Distribution of the poles in the closed-loop system considering the interaction between the SST and the APFs, after the modification of the APF controller where the SST mutual coupling is explicitly considered in the tuning process. Left) Distribution of all the poles in the complex plane; Right) Zoom around the imaginary axis.

poles of the system is provided in Fig. 9. As can be seen, compared to the previous poles distribution of Fig. 8, in this case all the poles of $S_A(s)$ and $S_M(s)$ (numerically computed from (12)-(13) in MATLAB) are located in the left-half side of the complex domain, indicating that the updated APF controller tuning should guarantee the closed-loop stability.

This has been verified experimentally on the PETT, and the results are shown in Fig. 10. After the activation of all the APF units, the second-order harmonic ripple in the DC-bus voltage is properly neutralized and, although the dynamics of the APFs is slower if compared to the previous tuning criterion (e.g., if compared to Fig. 2), there is no insurgence of instability caused by the mutual interactions in the SST, contrarily to how it was happening in the previous results shown in Fig. 3.

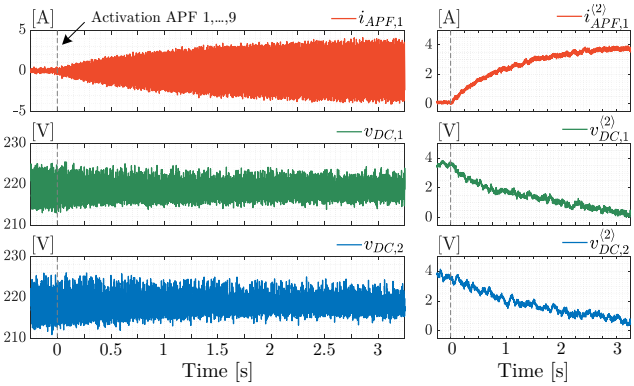


Fig. 10. Experimental results showing the simultaneous activation of all APFs after the modification of the APF controller where the SST mutual coupling is explicitly considered in the tuning process.

## V. Conclusions

ISOP SST converters are subject to a second-order harmonic ripple caused by the local single-phase AC/DC conversion in each module. This ripple can be counteracted by installing active power filters. However, the ISOP configuration is subject to mutual coupling between different modules, and the operation of the APFs may be subject to unexpected mutual interactions, potentially leading to instability. These aspects have been investigated in this work, considering the special example of the Power Electronics Traction Transformer.

It has been shown from experimental observations that guaranteeing the stability of a single APF in operation is not enough to automatically guarantee a stable behavior when multiple APFs are enabled at once. Instead, stronger requirements are needed. To properly analyze this phenomenon, the ISOP SST has been modeled as a multi-port network and represented mathematically through an equivalent impedance matrix, which intrinsically considers the effects of the coupling among different modules.

This coupling can influence the behavior of the APFs, both in open-loop and in closed-loop operation. For the open-loop scenario, it has been shown that the operation of a single APF unit can be extremely different from the operation of multiple APFs at once. For the closed-loop scenario, it has been shown that the stability depends on the interaction between the impedance matrix of the SST and the admittance implemented by control in the APF. In this case, the distribution of the poles in the closed-loop system can be affected according to the number of APF units in operation.

These effects should be properly considered in the design stage, in a way to improve the reliable operation of ISOP SSTs. These results will be used in future works to provide easier analysis tools and design guidelines for ISOP SSTs equipped with APFs.

## References

[1] J. E. Huber and J. W. Kolar, "Solid-State Transformers: On the Origins and Evolution of Key Concepts," in IEEE Industrial Electronics Magazine, vol. 10, no. 3, pp. 19-28, Sept. 2016, doi: 10.1109/MIE.2016.2588878.

[2] E. R. Ronan, S. D. Sudhoff, S. F. Glover and D. L. Galloway, "A power electronic-based distribution transformer," in IEEE Transactions on Power Delivery, vol. 17, no. 2, pp. 537-543, April 2002, doi: 10.1109/61.997934.

[3] M. Liserre, G. Buticchi, M. Andresen, G. De Carne, L. F. Costa and Z. X. Zou, "The Smart Transformer: Impact on the Electric Grid and Technology Challenges," in IEEE Industrial Electronics Magazine, vol. 10, no. 2, pp. 46-58, June 2016, doi: 10.1109/MIE.2016.2551418.

[4] D. Dujic et al., "Power Electronic Traction Transformer-Low Voltage Prototype," in IEEE Transactions on Power Electronics, vol. 28, no. 12, pp. 5522-5534, Dec. 2013, doi: 10.1109/TPEL.2013.2248756.

[5] J. Wei, Y. Wang, S. Liu, H. Feng and L. Ran, "Reliability-oriented design of DC-link considering the second-order harmonic current routing in an SST cell," in CPSS Trans. Pow. Electron. and Appl., doi: 10.24295/CPSSTPEA.2023.00025.

[6] Y. Sun, Y. Liu, M. Su, W. Xiong and J. Yang, "Review of Active Power Decoupling Topologies in Single-Phase Systems," in IEEE Trans. Pow. Electron., vol. 31, no. 7, pp. 4778-4794, July 2016, doi: 10.1109/TPEL.2015.2477882.

[7] D. Neumayr, G. C. Knabben, E. Varescon, D. Bortis and J. W. Kolar, "Comparative Evaluation of a Full- and Partial-Power Processing Active Power Buffer for Ultracompact Single-Phase DC/AC Converter Systems," in IEEE Journ. Emerg. Select. Topics in Pow. Electron., vol. 9, no. 2, pp. 1994-2013, April 2021, doi: 10.1109/JESTPE.2020.2987937.

[8] Z. Qin, Y. Tang, P. C. Loh and F. Blaabjerg, "Benchmark of AC and DC Active Power Decoupling Circuits for Second-Order Harmonic Mitigation in Kilowatt-Scale Single-Phase Inverters," in IEEE Journ. Emerg. Select. Topics in Pow. Electron., vol. 4, no. 1, pp. 15-25, March 2016, doi: 10.1109/JESTPE.2015.2490199.

[9] A. Cervone, T. Wei and D. Dujic, "Coupling Dynamics of Second-Order Harmonic Active Filters in Single-Phase Input-Series/Output-Parallel AC-DC Converters," PCIM Europe 2023, Nuremberg, Germany, 2023, pp. 1-10, doi: 10.30420/566091033

[10] C. Zhao et al., "Power Electronic Traction Transformer—Medium Voltage Prototype," in IEEE Transactions on Industrial Electronics, vol. 61, no. 7, pp. 3257-3268, July 2014, doi: 10.1109/TIE.2013.2278960.

[11] N. Hugo, P. Stefanutti, M. Pellerin and A. Akdag, "Power electronics traction transformer," 2007 European Conference on Power Electronics and Applications, Aalborg, Denmark, 2007, pp. 1-10, doi: 10.1109/EPE.2007.4417649.

[12] T. Wei, A. Cervone and D. Dujic, "Second Harmonic Ripple Voltage Suppression for Single-Phase ISOP Solid-State Transformer by Active Power Decoupling," 2023 IEEE Applied Power Electronics Conference and Exposition (APEC), Orlando, FL, USA, 2023, pp. 1496-1502, doi: 10.1109/APEC43580.2023.10131324.

[13] A. Cervone, T. Wei and D. Dujic, "Fourier-Based Harmonic Control of Plug-and-Play Active Filters for Input-Series/Output-Parallel Solid-State Transformers," IECON 2023, Singapore, 2023

[14] J. E. Huber, J. Minibock and J. W. Kolar, "Generic Derivation of Dynamic Model for Half-Cycle DCM Series Resonant Converters," in IEEE Trans. Pow. Electron., vol. 33, no. 1, pp. 4-7, Jan. 2018, doi: 10.1109/TPEL.2017.2703300.